



## Hydrogen storage by physisorption: beyond carbon

Seung-Hoon Jhi, Young-Kyun Kwon\*, Keith Bradley\*, Jean-Christophe P. Gabriel

*Nanomix Inc., Computational Materials Design, 5980 Horton Street, Suite 600, Emeryville, CA 94608, USA*

Received 21 November 2003; received in revised form 18 December 2003; accepted 23 December 2003 by S.G. Louie

### Abstract

Hydrogen storage using physisorption requires higher desorption temperatures than those possible using conventional adsorbents such as carbon. Using computational design, we predict that several materials have extremely strong physisorption interactions with hydrogen, including 12 kJ/mol heat of adsorption for hydrogen on some sites. Experimental adsorption isotherms on one of the materials, boron oxide, confirm the calculations, and large coverage is observed at temperatures as high as the boiling point of methane, 115 K. Since these materials have  $sp^2$ -like bonding, they should be amenable to the rich variety of chemical manipulations that have been used with carbon.

© 2004 Elsevier Ltd. All rights reserved.

PACS: 61.46. + w; 68.43. – h; 84.60.Ve

Keywords: A. Boron oxides; A. Nanostructured materials; D. Hydrogen storage; D. Physisorption

Hydrogen storage is a significant challenge to the large-scale use of hydrogen as an energy medium, because compressed hydrogen and liquid hydrogen have serious drawbacks [1]. The intriguing alternative of hydrogen storage in a material has led to metal hydrides [2], chemical hydrides [3], and physisorption-based storage [4]. However, none of these approaches has yet achieved both goals of high hydrogen capacity and moderate desorption temperature,  $T_D$ . In the case of physisorption, the hydrogen capacity of a material is proportional to its specific surface area [5–7]. Great progress has been made in providing materials with high capacities [8–11], including carbon with a surface area of 2600  $m^2/g$  and the capacity to adsorb 30 mmol/g of hydrogen [4] (corresponding to 5.8% by weight). However, practical application of these materials has been limited by low values of  $T_D$ , with even the best example, carbon, releasing hydrogen at 80 K, far from the goal of 200 K. This property is a fundamental effect of the interaction between hydrogen and the adsorbent material, and it has proven

difficult to achieve higher values by modifying carbon. Here we predict that several non-carbon light-element compounds have higher  $T_D$  than carbon, and we demonstrate 30% higher  $T_D$  for boron oxide.

Past approaches to increase  $T_D$  have attempted to take advantage of the strong interactions of hydrogen with alkali and transition metals. A central problem is that metal atoms, while they increase  $T_D$ , simultaneously increase the density of adsorbent material; thus only limited quantities of metals can be added without degrading the hydrogen capacity. For example, activated carbon was modified by the inclusion of 1% transition metal impurities [12] to produce minor increases in  $T_D$ . Similar approaches in carbon nanotubes have yielded spectacular improvements [13–15], but these results have not been reproduced [16–18]. We have searched for materials containing only light elements on which hydrogen adsorbs with high  $T_D$ . We report the prediction and experimental confirmation of non-graphitic materials for hydrogen physisorption with 30% higher  $T_D$  (as high as 115 K) than carbon. The finding of these strong physisorbents represents a milestone in the development of new classes of porous adsorbents for hydrogen storage at convenient temperatures.

The value of  $T_D$  is determined by the strength of the

\* Corresponding authors. Tel.: +1-5104285311; fax: +1-5106580425.

E-mail addresses: [shjhi@nano.com](mailto:shjhi@nano.com) (S.H. Jhi), [ykkwon@nano.com](mailto:ykkwon@nano.com) (Y.K. Kwon), [kbradley@nano.com](mailto:kbradley@nano.com) (K. Bradley), [jcgabriel@nano.com](mailto:jcgabriel@nano.com) (J.C.P. Gabriel).

interaction between hydrogen and a material's surface, called the heat of adsorption,  $Q_s$ . We have performed extensive computational simulations to identify three materials with high heats of adsorption for hydrogen. We selected for calculation compounds which form  $sp^2$ -like bonds, similar to graphite, because they are expected to avoid strong chemical reactions with adsorbates but retain substantial molecular binding. In order to estimate the heat of adsorption of hydrogen on candidate materials, a series of total energy calculations based on ab initio pseudopotential density functional methods were performed [19]. Computation by these methods can predict key physical properties of materials such as crystal structure, electronic and optical properties, transport properties, and gas adsorption kinetics. Details of the calculations are following. To simulate hydrogen sorption on model materials, a large section of the adsorbent host material, shown in Fig. 1a, is computationally depicted in an infinitely repeated lattice. The total energy of the combined system (adsorbents and  $H_2$ ) is then calculated using varying distances between  $H_2$  and the adsorbents. Atomic orbitals with double- $\zeta$  polarization are used for the expansion of single-particle wavefunctions [20]

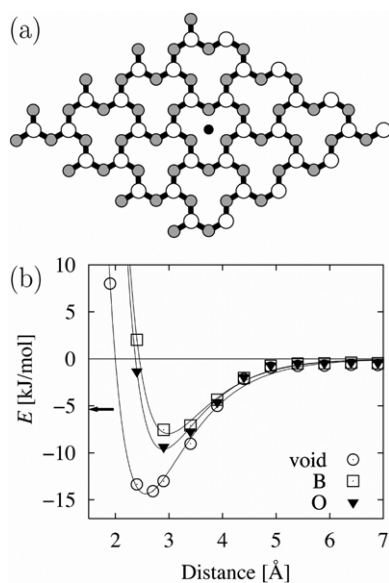


Fig. 1. (a) Top view of a  $B_2O_3$  layer. Empty and grey circles represent boron and oxygen atoms, respectively. Solid circle denotes a hydrogen molecule with its axis perpendicular to the layer, over the center of a boroxol ring. (b) Energy versus distance from the boron oxide surface for hydrogen located over various sites. Each data set of the calculated energy has been fit with the Morse function. The minima of the curves represent the heats of adsorption of the hydrogen molecules at these sites, including voids (empty circles), oxygen atoms (solid inverse triangle), and boron atoms (empty squares). The heats of adsorption on these sites are averaged, weighted by area, to provide the heat of adsorption for hydrogen on boron oxide reported in the text. For comparison, the arrow indicates the heat of adsorption of hydrogen on carbon, which depends only weakly on which site the hydrogen is over.

with the cut-off energy of 80 Ry. We use 0.01 Ry of the confinement energy shift, which defines the cut-off radii of the atomic orbitals. The exchange-correlation interaction of electrons is treated with a generalized gradient approximation approach [21], which is known to be superior to the local density approximation for describing the interaction of gas molecules with solid surfaces. At each step of the total energy calculation, a full range of structural relaxations is carried out under the constraint of a fixed distance between  $H_2$  and adsorbents until their Hellmann–Feynman forces are less than  $0.001 \text{ Ry}/a_0$ , where  $a_0$  is the Bohr radius. Once a set of values for the total energy as a function of the distance between  $H_2$  and adsorbents has been calculated, the data are fit with Morse function, as shown in Fig. 1b. The minimum total energy corresponding to the heat of adsorption, and the binding distance, at which the minimum occurs, are then obtained. For some materials, the heat of adsorption is often different for different adsorption sites. In these cases, we calculate an average heat of adsorption weighted by the area of each adsorption site.

Our calculation for the heat of adsorption of hydrogen on carbon is about 6 kJ/mol [22], in good agreement with recent measurements done on activated carbons [23], confirming the accuracy of the method. Among our heat of adsorption calculations on various other materials, we have identified three substances as strong hydrogen adsorbers, with heats of adsorption ranging from 9 to 12 kJ/mol. These values represent the strong binding of hydrogen on these materials, while their corresponding binding distances, as shown in Fig. 1b, indicate that their interactions are still of the physisorption type. This strong binding results from the polarities of the bonds in these materials.

The compound  $\beta\text{-C}_3\text{N}_4$ , with a heat of adsorption for hydrogen of 11 kJ/mol, has been predicted to have a bulk modulus comparable to diamond [24], but it has only been observed in nanocrystalline forms at very low yields [25, 26].  $\text{BeB}_2$ , with a heat of hydrogen adsorption of 9 kJ/mol, is a layered material that may form nanotubes similar to carbon nanotubes [27]. However, the inclusion of beryllium, a toxic element, prevents the wide application of  $\text{BeB}_2$  as a hydrogen storage material. The third substance,  $B_2O_3$ , with a heat of hydrogen adsorption of 12 kJ/mol, is an important industrial mineral which occurs most often in a glass-like structure [28,29]. Although its phase diagram is complex, particularly in the presence of water, the boroxol rings, shown in Fig. 1a, which we have used in our calculation, are ubiquitous.

Given these considerations, from the candidate compounds we chose  $B_2O_3$  for hydrogen adsorption measurements. To measure the adsorption properties of the  $B_2O_3$  surface, without enhancement by coordination effects, we prepared fine powders of  $B_2O_3$ . Freeze drying of boric acid solution at  $-10^\circ\text{C}$  produced powders with surface areas up to  $20 \text{ m}^2/\text{g}$ , of which TEM image is shown in Fig. 2. These powders contain many nanoparticles, but do not contain

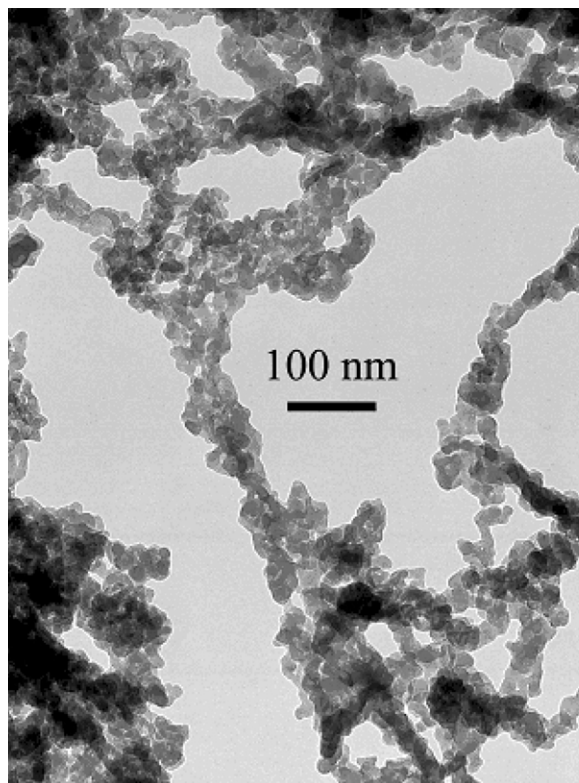


Fig. 2. Transmission electron micrograph of boron oxide particles. These materials are fine powders with sizes between 10 and 100 nm and specific surface areas of tens of  $\text{m}^2/\text{g}$ . The surface area is commensurate with the observed particle sizes, suggesting that the particles are not porous.

porous features; there are no crevices or slit-pores for preferential adsorption. Other non-porous preparations, including condensation of nanoparticles from boron oxide vapor, produced materials with similar hydrogen storage properties.

The powders were transferred from an argon atmosphere to a Micromeritics ASAP 2010 porosimeter for gas adsorption measurements. Multiple nitrogen and hydrogen adsorption isotherms were measured, with in situ degassing between measurements. The degas protocol was chosen with regard to the boric acid phase changes [28,29], identified by thermogravimetric analysis at 90, 140 and 190 °C. Samples in  $10^{-4}$  Torr vacuum were heated in steps, with the temperature held at each level for 4 h (8 h at 190 °C). The adsorption volumes were in 1/4" OD glass tubes with 10 cc bulbs. Temperatures were maintained by fixed point baths, including boiling nitrogen and argon and several slushes of organic solvents. After each gas adsorption isotherm, the sample tube was evacuated for 30 min in the isothermal bath. After evacuation the free space was measured using helium at the bath temperature. Multiple runs were performed at each temperature to measure uncertainty. In

addition, for some runs helium free space measurements were made before the isotherms to verify that free space values were stable. The volumetric method was chosen because it is much less susceptible, than gravimetric methods, to mistaking impurity adsorption for adsorption of hydrogen [16].

We compared boron oxide samples to an acetylene carbon black (Alfa Aesar, 99.9%) which has similar surface area ( $80 \text{ m}^2/\text{g}$ ), particle size, and porosity, as inferred from TEM images (Fig. 2) and nitrogen adsorption isotherms shown in the inset of Fig. 3. The quantity plotted for the nitrogen adsorption, the specific adsorption, indicates the quantity of nitrogen taken up by 1 g of each material. Because the carbon has a higher surface area, it takes up more nitrogen. Similarly, having more surface area it takes up more hydrogen per gram. The hydrogen adsorption, shown in Fig. 3, has been normalized by the surface areas, measured by the nitrogen adsorption with BET analysis [30], to measure the fractional surface coverage by hydrogen in moles per area. Although neither sample reaches full coverage in the pressure range studied, the

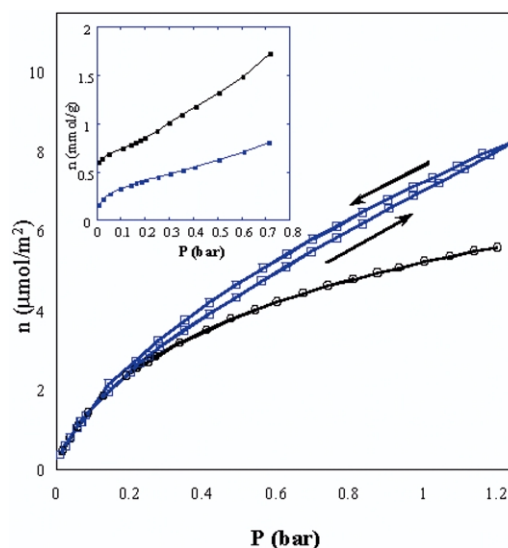


Fig. 3. Hydrogen sorption isotherms at 77 K for boron oxide (empty squares) and carbon (empty circles). Since the two samples have different surface areas, they adsorb different absolute quantities of hydrogen. To compare them, the quantity of hydrogen adsorbed has been normalized by the sample surface areas. The resulting data, measured in moles per area, represent what fraction of the sample surfaces are covered by adsorbed hydrogen. For boron oxide, both adsorption and desorption isotherms are plotted, as indicated by the arrows. Inset shows nitrogen adsorption isotherms for boron oxide (lower curve) and carbon (upper curve) at 77 K, in units of moles per gram of each material. Nitrogen uptake is assumed to be proportional to surface area, and these isotherms are used to calculate the surface areas for the two materials by BET analysis [30]. Note also that the shapes of the isotherms, which are of Type I [30] with no plateau or adsorption hysteresis, is consistent with the low porosity of the materials.

hydrogen capacity of surfaces is known to be  $11 \mu\text{mol}/\text{m}^2$  [23]. Thus, the data in Fig. 3 show boron oxide adsorbing 75% of full coverage, while carbon adsorbs only 50% of full coverage; the greater coverage is the result of the higher heat of adsorption. The adsorption was fully reversible, indicating that the gas was physisorbed.

The desorption temperature  $T_D$  can be extracted from the temperature dependence of adsorption coverage, again normalized by surface area and is shown in Fig. 4. To reach a coverage of  $4 \mu\text{mol}/\text{m}^2$  at 1 bar requires 80 K for carbon and 110 K for boron oxide. Thus, while  $T_D$  is 80 K for carbon, comparable to the boiling point of nitrogen,  $T_D$  is 110 K for boron oxide, comparable to the boiling point of natural gas. To estimate  $Q_s$ , the isosteric heat of adsorption, we observe that the coverage  $\theta$  (in  $\mu\text{mol}/\text{m}^2$ ) follows an Arrhenius-type law [30], with

$$\theta \propto \exp\left(-\frac{Q_s}{kT}\right). \quad (1)$$

Thus by comparing the temperatures  $T_{\text{Carbon}}$  and  $T_{\text{B}_2\text{O}_3}$  required to reach a fixed coverage, we conclude that

$$\frac{Q_{\text{Carbon}}}{Q_{\text{B}_2\text{O}_3}} = \frac{T_{\text{Carbon}}}{T_{\text{B}_2\text{O}_3}} \quad (2)$$

at that coverage. Using the data in Fig. 4, we find that boron oxide has a binding energy higher than carbon by 30% for coverages between 2 and  $6 \mu\text{mol}/\text{m}^2$ . Thus the experimental heat of adsorption is 8 kJ/mol, in good agreement with the theoretical prediction, especially considering that intermediate coverages involve primarily the boron and oxygen sites.

The materials discussed here provide broad opportunities

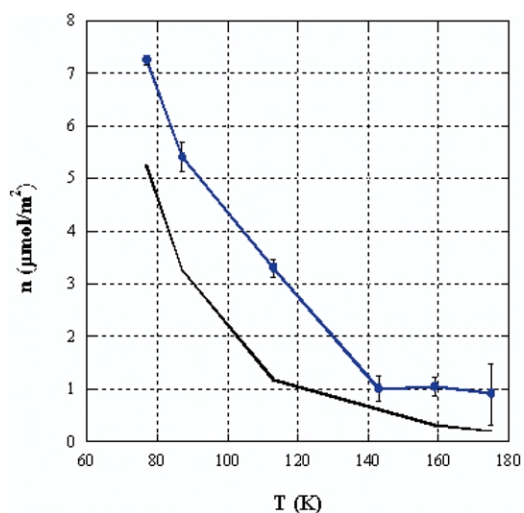


Fig. 4. Hydrogen adsorption isobars at 1 bar for boron oxide (upper curve) and carbon (lower curve). The quantity of hydrogen adsorbed has been normalized by sample surface area, as in Fig. 3. The temperature dependence of hydrogen adsorption is used to observe  $T_D$  and to estimate the heat of adsorption. Hydrogen remains adsorbed on boron oxide at higher temperatures than on carbon.

for manipulation and modification. In particular, boron oxide chemistry is as rich as that of carbon [29]. Thus, these materials represent the first examples of a new class of strong hydrogen sorbents, discovered through an efficient feedback between theory and experiment. Compared to carbon, they have higher heats of adsorption for hydrogen, although the interaction continues to be primarily physisorptive. Hydrogen can thus be stored on these materials with 30% higher  $T_D$  than on carbon. We anticipate new research to explore this new area, physisorption on non-carbon light-element compounds, with the extensive techniques developed for carbon sorbents.

#### Acknowledgements

We thank George Gruner, Steven G. Louie, Marvin L. Cohen, and Alex Zettl for helpful discussions. We acknowledge M.R. Gardiner for assistance with the measurements and S. Kwan and J. Sprunck for assistance with sample preparation. Transmission electron microscopy was performed by M.V.P. Altoe using the National Center for Electron Microscopy.

#### References

- [1] L. Schlappbach, A. Zuttel, *Nature* 414 (2001) 353–358.
- [2] R.L. Cohen, J.H. Wernick, *Science* 214 (1981) 1081–1087.
- [3] P. Chen, Z. Xiong, J. Lou, J. Lin, K.L. Tan, *Nature* 420 (2002) 302–304.
- [4] H. Marsh, D. Crawford, T.M. O’Grady, A. Wennerberg, *Carbon* 20 (1982) 419–426.
- [5] M. Rzepka, P. Lamp, M.A. De La Casa-Lillo, *J. Phys. Chem. B* 102 (1998) 10894–10898.
- [6] A. Csaplinski, E. Zielinski, *Przem. Chem.* 37 (1958) 640.
- [7] A. Herbst, P. Harting, *Adsorption* 8 (2002) 111–123.
- [8] M. Eddaoudi, J. Kim, N. Rosi, D. Vodak, J. Wachter, M. O’Keefe, O.M. Yaghi, *Science* 295 (2002) 469–472.
- [9] P.D. Yang, T. Deng, D.Y. Zhao, P.Y. Feng, D. Pine, B.F. Chmelka, G.M. Whitesides, G.D. Stucky, *Science* 282 (1998) 2244.
- [10] N.F. Zheng, X.G. Bu, B. Wang, P.Y. Feng, *Science* 298 (2002) 2366–2369.
- [11] J. Weitkamp, M. Fritz, S. Ernst, *Int. J. Hydrogen Energy* 20 (1995) 967–970.
- [12] J.S. Noh, R.K. Agarwal, J.A. Schwarz, *Int. J. Hydrogen Energy* 12 (1987) 693–700.
- [13] C. Liu, Y.Y. Fan, M. Liu, H.T. Cong, H.M. Cheng, M.S. Dresselhaus, *Science* 286 (1999) 1127–1129.
- [14] A.C. Dillon, K.M. Jones, T.A. Bekkedahl, C.H. Kiang, D.S. Bethune, M.J. Heben, *Nature* 386 (1997) 377–379.
- [15] P. Chen, X. Wu, J. Lin, K.L. Tan, *Science* 285 (1999) 91–93.
- [16] F.E. Pinkerton, B.G. Wicke, C.H. Olk, G.G. Tibbetts, G.P. Meisner, M.S. Meyer, J.F. Herbst, *J. Phys. Chem. B* 104 (2000) 9460–9467.
- [17] R.T. Yang, *Carbon* 38 (2000) 623–626.
- [18] M. Hirscher, M. Becher, M. Haluska, U. Dettlaff-Wegli-

- kowska, A. Quintel, G.S. Duesberg, Y.M. Choi, P. Downes, M. Hulman, S. Roth, I. Stepanek, P. Bernier, *Appl. Phys. A-Mater.* 72 (2001) 129–132.
- [19] M.L. Cohen, *Phys. Scripta T1: 5-10 (Sp. Iss. SI)* (1982).
- [20] D. Sanchez-Portal, P. Ordejon, E. Artacho, J.M. Soler, *Int. J. Quantum Chem.* 65 (1997) 453.
- [21] J.P. Perdew, K. Burke, M. Ernzerhof, *Phys. Rev. Lett.* 77 (1996) 3865.
- [22] Y.-K. Kwon, S.-H. Jhi, to be published.
- [23] P. Benard, R. Chahine, *Langmuir* 17 (2001) 1950.
- [24] A.Y. Liu, M.L. Cohen, *Phys. Rev. B* 41 (1990) 10727.
- [25] Y. Fahmy, T.D. Shen, D.A. Tucker, R.L. Spontak, C.C. Koch, *J. Mater. Res.* 14 (1999) 2488.
- [26] L.W. Yin, M.S. Li, Y.X. Liu, J.-L. Sui, J.M. Wang, *J. Phys. Condens. Mater.* 15 (2003) 309.
- [27] P.H. Zhang, V.H. Crespi, *Phys. Rev. Lett.* 89 (2002) 056403.
- [28] L.M. Anovitz, B.S. Hemingway, *Rev. Mineral.* 33 (1996) 181–261.
- [29] N.N. Greenwood, A. Earnshaw (Eds.), *Chemistry of the Elements*, Butterworth-Heinemann, Oxford, 1997.
- [30] E. Alison Flood (Eds.), *The Solid-gas Interface*, Marcel Dekker, New York, NY, 1966.